Journal of Advanced Research 82 (2026) 751–764

Contents lists available at ScienceDirect

Journal of Advanced Research

journal homepage: www.elsevier.com/locate/jare

Original Manuscript

Transglutaminase 2 modulates inflammatory angiogenesis via vascular endothelial growth factor receptor 2 pathway in inflammatory bowel disease

Gaoshi Zhou [a,1], Mudan Zhang [a,1], Shuhui Zheng [b,1], Guang Yang [c,1], Li Li [a], Shanshan Huang [a], Zhirong Zeng [a], Rirong Chen [a,*], Shenghong Zhang [a,d,*], Minhu Chen [a,e,*]

[a] *Department of Gastroenterology, The First Affiliated Hospital, Sun Yat-sen University, Guangzhou, PR China*
[b] *Research Center for Translational Medicine, The First Affiliated Hospital, Sun Yat-sen University, Guangzhou, PR China*
[c] *Department of Minimally Invasive Intervention, State Key Laboratory of Oncology in South China, Guangdong Provincial Clinical Research Center for Cancer, Sun Yat-sen University Cancer Center, Guangzhou, PR China*
[d] *Guangxi Hospital Division of The First Affiliated Hospital, Sun Yat-sen University, Nanning, PR China*
[e] *Department of Gastroenterology, Shenzhen Qianhai Taikang Hospital, Shenzhen, PR China*

HIGHLIGHTS

- Expression of TGM2 is significantly increased in enteric endothelial cells of patients with IBD.
- TGM2 enhances VEGFR2 phosphorylation via interaction with VEGFR2 to promote inflammatory angiogenesis.
- TGM2 knockout and its inhibitor significantly attenuate colitis and angiogenesis in mice.
- TGM2 is a reliable serum biomarker for assessing endoscopic disease activity in patients with CD.

GRAPHICAL ABSTRACT

Graphic abstract showing TGM2 modulates inflammatory angiogenesis via vascular endothelial growth factor receptor 2 pathway in inflammatory bowel disease and TGM2 inhibition served as potential therapeutic target for IBD.

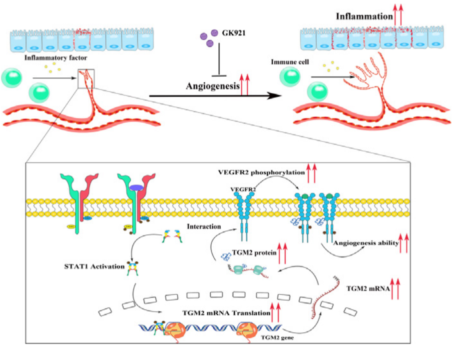

ARTICLE INFO

Article history:
Received 2 April 2025
Revised 23 June 2025
Accepted 2 July 2025
Available online 4 July 2025

Keywords:
Transglutaminase 2
Inflammatory bowel disease
VEGFR2
Angiogenesis

ABSTRACT

Objectives: Immune-driven inflammatory angiogenesis is a crucial component in the pathogenesis of inflammatory bowel disease (IBD). Nevertheless, the underlying mechanisms are still poorly understood. This study aims to investigate the role of Transglutaminase 2 (TGM2) in inflammatory angiogenesis in IBD and its potential as a therapeutic target and biomarker.
Methods: We performed an RNA-seq analysis integrated single-cell transcriptomic profiling on IBD biopsies to identify dysregulated genes. Additionally, we explored TGM2 contribution to angiogenesis and colitis under in vitro and in vivo conditions in *Tgm2* knockout mouse and human intestinal microvascular endothelial cells (HIMECs). Serum TGM2 levels were measured by Enzyme-Linked Immunosorbent Assay.
Results: TGM2 expression was significantly upregulated in intestinal endothelial cells of IBD patients and colitis models. *Tgm2* knockout and its inhibitor significantly attenuated intestinal colitis and angiogenesis in mice. In vitro, knockdown of TGM2 significantly suppressed tube formation, migration, and invasion of

---

* Corresponding authors at: M.D. 58 Zhongshan Road 2, Guangzhou 510080, PR China.
E-mail addresses: chenrr9@mail2.sysu.edu.cn (R. Chen), zhshh3@mail.sysu.edu.cn (S. Zhang), chenminhu@mail.sysu.edu.cn (M. Chen).

[1] These authors contributed equally to this work.

https://doi.org/10.1016/j.jare.2025.07.002

HIMECs. Mechanistically, inflammation-induced STAT1 activation promoted TGM2 expression, which subsequently interacted with vascular endothelial growth factor receptor 2 (VEGFR2) to drive its phosphorylation (Tyr1059, Tyr1214) and inflammatory angiogenesis. In patients of Crohn's Disease, serum TGM2 concentrations exhibited high diagnostic accuracy (AUC = 0.862) for assessing endoscopic activity.

Conclusion: Our findings underscore the critical role of STAT1-TGM2-VEGFR2 axis in regulating angiogenesis during intestinal inflammation, suggesting that targeting TGM2 as a viable therapeutic candidate for vascular remodeling in chronic intestinal inflammation.

Introduction

Inflammatory bowel disease (IBD) is a recurrent chronic inflammatory intestinal disorder with a multifactorial etiology that encompassing Crohn's disease (CD) and ulcerative colitis (UC) [1,2]. Despite the widespread use of small-molecule drugs and biologic agents in management of IBD, a wide subset of patients fails to achieve an adequate therapeutic response due to treatment intolerance or primary and secondary non-response, requiring novel therapeutic strategies [3,4]. Active angiogenesis is noted in both IBD and experimental colitis models during mucosal cell regeneration, and tissue remodeling correlates with disease activity [5,6]. Accumulating evidence proposes immune-driven inflammatory angiogenesis as crucial to the pathogenesis of IBD [7,8]. Angiogenesis has a pivotal role in facilitating nutrient delivery and eliminating cellular metabolic waste during initial mucosal healing phases in IBD [9,10]. Inflammatory factors released from the inflamed mucosa contribute to tissue damage and pathological angiogenesis [11]. Nevertheless, our insights into angiogenesis-mediated chronic inflammation continue to evolve, and whether targeting angiogenesis could be a therapeutic potential in IBD management requires further in-depth investigation [12].

The mammalian transglutaminase (TG) family consists of eight highly-conserved multi-functional isoenzymes that catalyze the calcium (Ca^{2+})-dependent post-translational modification by covalently cross-linking a primary amine group to the γ-carboxamide groups of peptide-bound glutamines [13,14]. Among the members of the TG family, transglutaminase 2 (TGM2), comprising 686 amino acids with a four-domain structure, is the most ubiquitous isoenzyme and functions as a transglutaminase, Ca^{2+}-independent GTPase, protein disulfide isomerase, scaffolding protein, and protein kinase [14,15]. Aberrant TGM2 activation has been mechanistically linked to multiple pathogenic human conditions, including cancer, cardiovascular diseases, and fibrosis [14]. TGM2 is also involved in pathological angiogenesis [16,17]. Increased TGM2 expression was observed in the intestinal mucosal epithelium of patients with IBD [18]. Utilizing RNA sequencing and integrated single-cell transcriptomic analysis, we observed a significant upregulation in TGM2 expression within intestinal endothelial cells of patients with IBD. Nevertheless, the findings of studies examining the role of TGM2 in colitis models are contradictory [19,20]. Despite previous efforts, the underlying role of TGM2 in IBD pathogenesis remains elusive, and the association between TGM2 and the clinical characteristics of IBD has rarely been studied.

Here, we aimed to elucidate the role and mechanism of TGM2 in angiogenic activation during inflammation in patients with IBD and evaluate whether targeting TGM2 could serve as a potential anti-angiogenic therapeutic option for IBD.

Material and methods

Human sample collection

All human serum samples and colonic biopsy tissues were obtained from healthy individuals and patients with IBD underwent routine endoscopy at the First Affiliated Hospital of Sun Yat-sen University (Guangzhou, China) from 2017 to 2021. Patients with IBD were diagnosed following the European Crohn's and Colitis Organization guidelines [21]. This study received approvals from ethics committees, and all participants have signed written informed consent ([2019] No. 084). The demographics and clinical data of the included patients, including Serum CRP, PLT, and ESR measured by the Department of Medical Laboratory, were collected and statistically analysed. Crohn's Disease Endoscopic Index of Severity (CDEIS) was assessed in accordance with guidelines [22,23].

RNA-SEQ analysis

Human colonic samples were obtained from healthy individuals (n = 18) and patients with Crohn's disease (CD, n = 11) and ulcerative colitis (UC, n = 9) for transcriptome sequencing (OE Biotech, Shanghai, China). RNA samples were extracted by TRIzol reagent (Invitrogen, USA). cDNA libraries were synthesized from RNA samples utilizing the TruSeq RNA Library Prep Kit (Illumina, USA) and then sequenced on an Illumina HiSeq. Publicly available RNA-seq datasets (GSE95095 and GSE243625) were obtained from GEO database. All RNA-seq data were processed and analyzed using ExpressAnalysis [24].

Single-cell sequencing analysis

Data regarding 75 samples of patients with IBD and healthy tissues were collected from four GEO datasets (GSE134809 [25], GSE202052 [26], GSE214695 [27], and GSE231993 [28]) used for single-cell sequencing analysis (scRNA-seq). R (version 4.3.3) was used to perform this study, and single-cell Seurat objects were processed through the Seurat package (version 5.1.0). Data frames and plots were processed through the Tidyverse package (version 2.0.0) [29,30]. Single cells were qualified based on the percentage of mitochondrial gene expression and annotated into seven major groups.

Mice strains

C57BL/6 mice and *Tgm2*-knockout C57BL/6 (Cat. NO. NM-KO-191051) were bred from Shanghai Model Organisms Company (SMOC, China). All animal experiments were executed using 6–10-week-old male mice maintained in the specific pathogen-free (SPF) facility in the Animal Laboratory of the First Affiliated Hospital of Sun Yat-sen University. The paired sgRNA sequences (5′-3′) were as follows:

Tgm2 gRNA1 GAAGGCCTTAATTCCACCTC PAM: CGG
Tgm2 gRNA2 AGGGTTCCTCCAGTGCCCGG PAM: AGG
Tgm2 gRNA3 GCTAGCCTGTGCTCACCATG PAM: AGG
Tgm2 gRNA4 AGGACAGTCCCTGCCCCTCA PAM: TGG

Acute colitis models

Acute colitis models were established as described previously [31]. Briefly, for acute DSS-induced colitis, animals were given 2.5 % dextran sodium sulfate (DSS, MP Biomedicals, USA) dissolved in sterile water for 7 days. Control mice received sterile water alone. Disease progression was monitored daily by evaluating weight loss, stool consistency, occult blood, and rectal bleeding. The scoring system for disease activity index (DAI) were given based on parameters involving weight loss, stool consistency, and stool blood level [31]. All mice were euthanized from days 9–11. For the acute trinitrobenzene sulfonic acid (TNBS) -induced colitis, animals were pre-sensitized with 100 μL of 1 % (w/v) TNBS (Sigma-Aldrich, USA) 7 days prior to induction. They were intrarectally administered 2.5 % TNBS solution (100 μL) in 50 % ethanol on the first day of model development. The mice were euthanized on days 2–3 according to the degree of inflammation. For the GK921 inhibitor experiment, mice received daily intraperitoneal injections of GK921 (10 mg/kg, MedChemExpress, USA). All experiments involving animal studies received approvals from the Ethics Committee ([2018] no. 039).

Histological score and MVD assessment

For morphological measurements, colonic sections were stained with HE. Images were captured by KfBio digital pathology scanner (KF-PRO-020, China). Histological scores were measured as previously described [31]. For MVD assessment, the vessels were highlighted with CD31 and MVD were counted at 400 × magnification in 3 regions in each colon section.

Isolation and culture of human intestinal microvascular endothelial cells (HIMECs)

HIMECs were isolated from the colonic tissues of fresh IBD surgical specimens as previously reported [32]. Briefly, dissected tissues were rinsed in sterile Hank's balanced salt solution (HBSS) and agitated for 15 min in HBSS containing 1 mM dithiothreitol to remove mucus. The epithelial cells were removed using a solution of 5 mM EDTA in HBSS for four sequential 30-min washes. After disaggregation of the tissue by rotating incubation with enzymatic digestion for 1 h, the cell suspension was filtered by 100-μm-pore nylon cell strainer (Biologix, China) thrice to remove tissue fragments, and a cell precipitate was collected by centrifugation. Further isolation by lymphocyte separation solution was performed to remove granulocytes and red blood cells. After centrifugation, the cells were resuspended and cultured overnight in RPMI containing 10 % fetal bovine serum (FBS) and 0.5 mM db-cAMP. Cells were then cultured with Endothelial Cell Medium (ECM, ScienCell, USA) and maintained at 37 ℃ in 5 % CO2. Further purification of HIMECs was performed using Dynabeads M-450 epoxy (Invitrogen, USA) coated with anti-CD31 antibodies (Invitrogen, clone HEC7). HIMECs were harvested between passages two and six after magnetic bead shedding.

Lentivirus infection and transfection

Lentiviruses were purchased from OBiO (Shanghai, China). HIMECs were transduced with an appropriate amount of lentivirus with 10 μg/mL polybrene as transfection enhancer. Cells were selected in 5 μg/mL of puromycin (Life Technologies, USA), and the infection efficacy of TGM2 was confirmed by subsequent analyses. The sequences of shRNA targeting *TGM2* were as follows: 5′-GGTCTGTGCACAAATCCAT-3′.

EdU proliferation assay

The Cell-Light EdU assay (RiboBio) was utilized in this experiment. HIMECs (5×10^5 cells/well) were seeded and labeled with 50 μM EdU for 2 h, followed by phosphate-buffered saline (PBS) washes. HIMECs were then fixed with paraformaldehyde (4 %) and was then neutralized with 2 mg/mL glycine. After permeabilization and washes, EdU staining and sealing were performed, and the results were observed using Leica DMi8 microscope (Germany).

Wound healing assay

A two-well Ibidi Silicone Culture Insert Chamber (Ibidi®, Germany) was placed on a 6-well plate, and HIMECs with *TGM2* knockdown and those with overexpression were then seeded into each well of culture inserts, followed by incubation until a confluent monolayer of cells was obtained. After achieving a conflluent monolayer, the culture inserts were carefully removed to establish a 500-μm cell-free gap, and the cell movement was monitored over the next 48 h. Images were captured at indicated time intervals with a Leica DMi8 microscope (Germany) to observe the migration and analyzed with ImageJ software.

Invasion assay

For invasion assays, Transwell® insert (8 μm PET membrane, 3428, Corning, USA) was coated with diluted Matrigel matrix. Subsequently, HIMECs with *TGM2* knockdown and those with overexpression and control HIMECs (5×10^4 cells) were seeded in the upper chambers in ECM without FBS and incubated overnight at 37 ℃. After PBS rinses, uninvaded cells were gently wiped and the migrated HIMECs were stained with crystal violet (Leagene), air-dried and imaged.

In vitro tube formation assay

An Ibidi μ-Slide 15 Well 3D (Ibidi®, Germany) was coated with Matrigel (356231, Corning, USA). HIMECs were pre-treated with 100 ng/mL IL-23 (PeproTech), 10 ng/mL IFN-γ (PeproTech), and 100 ng/mL IL-9 (PeproTech) for 48 h, followed by seeding 5×10^4-cells/well into Matrigel-coated wells. Inflammatory stimuli were maintained in the culture medium. After incubation for 24 h, the morphological changes and capacity of tube formation were observed and captured at different time points by an inverted phase contrast microscope. The studies were independently repeated in triplicate, with at least five fields were analyzed for each condition.

Extraction of total RNA and qRT-PCR

RNA samples from cells or tissues were extracted by the TRIzol reagent. The purity and concentration of RNA was measured using Nanodrop 2000. cDNA synthesis was conducted utilizing the Transcript First Stand cDNA Synthesis Kit (Roche, Basel, Switzerland). qRT-PCR analysis was carried out on LightCycler 480 machine (Roche). The relative quantification was performed using the $2^{-\Delta\Delta Ct}$ method. The primers used for qRT-PCR are listed in Supplemental Table S1.

Western blotting

Western blotting was conducted as previously mentioned [33]. Protein extraction was carried out with RIPA lysis buffer. After the protein concentration was determined, the protein lysates were electrophoresed on SDS-PAGE and transferred to PVDF membranes. Following blocking with 5 % BSA, membranes were incubated overnight at 4℃ with primary antibodies, including those targeting TGM2, VEGFR2, FAK, FLC-γ, P38 MAPK, P44/42 MAPK, and GAPDH and were subsequently incubated with secondary antibodies. Antibodies used are listed in Supplemental Table S2. Immunoblots were detected using the iBright™ FL1500 Imaging System and analysed for the grayscale of the bands using ImageJ software.

Immunohistochemistry (IHC) and immunofluorescence (IF) staining

For IHC, sections were incubated with antibodies targeting TGM2 (rabbit, CST), CD31 (mouse, CST), Ki-67 (rat, Thermo Scientific), and VEGFR2 (rabbit, CST) at 4 ℃ overnight. After 30 min of incubation with HRP-labelled secondary antibodies (CST, USA), slices were stained with DAB chromogen. Images were captured with KfBio digital pathology scanner (KF-PRO-020, China). For IF staining, tissues were incubated with indicated fluorescence-conjugated secondary antibodies (1:500, Thermo Scientific) for 1 h following the incubation of primary antibodies. Slices were mounted with Antifade reagent (Invitrogen, USA) and imaged by Olympus BX-63 microscope (Japan) or a THUNDER Imaging System (Leica, USA).

Immunoprecipitation

Immunoprecipitation was conducted using a Pierce Magnetic IP Kit (90409, Thermo Scientific) following the manufacturer's protocol. HIMECs with *TGM2* overexpression were grown to confluence on 100-mm Petri dishes. For each category, 2×10^7 cells were detached, collected, and resuspended in lysis buffer supplemented for protein extraction. Indicated IP antibodies or control IgG were added to the lysates and incubated at 4 °C overnight for antigen immunoprecipitation. The antigen–antibody complex was subsequently couple to Protein A/G magnetic beads (25 μL per reaction). After three washes, the immunoprecipitates were eluted and subjected to subsequent analysis.

Chromatin immunoprecipitation (ChIP) assay

SimpleChIP® Plus Enzymatic Chromatin IP assay (9005, CST, USA) was utilized in the experiment. Briefly, HIMECs were stimulated with IFN-γ (10 ng/mL) and then were crosslinked with 1 % formaldehyde. The cells were resuspended in ChIP lysis buffer and placed on ice for 10 min following neutralization and PBS washes. The antibody-protein complexes were immunoprecipitated using an anti-p-STAT1 antibody (9107, CST, USA) and control IgG. Among immunoprecipitation reaction, Protein A/G Magnetic Beads were added then and incubated at 4 °C for 2 h. The ChIP DNA fragments were amplified to target STAT1-binding motifs within the promoter region of the IFN-γ-encoding gene.

Enzyme-Linked Immunosorbent assay (ELISA)

Plasma TGM2 levels were quantified by ELISA (ELH-TGM2-1, RayBiotech, USA). The spectrophotometric absorbance of each sample was measured by Infinite M1000 microplate reader (Tecan) at 450 nm.

Statistical analysis

Statistical analyses were carried out utilizing GraphPad Prism 9.0 (GraphPad Software Inc., USA) or IBM SPSS (version 24.0), and the findings were displayed as mean ± SEM. The following thresholds were used to determine whether a difference was regarded as statistically significant: $p < 0.05$ (*), $p < 0.01$ (**), $p < 0.001$ (***), and $p < 0.0001$ (****). MedCalc software was used to perform ROC curve analysis (Version 16.8).

Results

Expression of TGM2 is increased in enteric endothelial cells of patients with IBD and mice with experimental colitis

The results from both gene array (Fig. 1A) and data from the Gene Expression Omnibus (GEO) database (Fig. 1B–C) demonstrated a marked upregulation of TGM2 expression in inflamed colonic tissues of patients with IBD. Furthermore, qPCR revealed a marked upregulation in *TGM2* mRNA levels in intestinal tissues of patients with IBD (Fig. 1D). Consistent with these findings, Western blot analysis further confirmed a substantial increase in TGM2 protein levels in the intestinal tissues of patients with IBD compared to those from normal group (Fig. 1G, H and I). Single-cell RNA sequencing data of GEO database highlighted a significant upregulation of TGM2, specifically in the endothelial cells of patients with IBD (Fig. 1L–M and S1). IHC and IF were used to elucidate the expression patterns of TGM2 in patients with IBD. The results showed a marked increase in blood vessel density along with heightened expression levels of TGM2, specifically within endothelial cells, in patients with IBD. However, no notable differences in TGM2 levels were observed in the subepithelial layers (Fig. 1N–O).

We further validated the expression of Tgm2 in the colonic tissues of mouse models of acute DSS and acute TNBS colitis mouse models. Both acute DSS and TNBS colitis models exhibited significantly increased mRNA and protein levels of Tgm2 (Fig. 1E–F and J–K). IHC and IF analyses also revealed a prominent upregulation of Tgm2 expression in endothelial cells, accompanied by enhanced blood vessel density in DSS-induced colitis. However, we observed only partial co-localization between Tgm2 and Cd31 within endothelial cells in the TNBS colitis model (Fig. 1P–Q). Therefore, mice with DSS-induced colitis displayed patterns of Tgm2 expression similar to those observed in patients with IBD.

TGM2 regulates the angiogenic ability of intestinal vascular endothelial cells

To investigate the association between increased TGM2 expression in the intestinal vascular endothelial cells of patients with IBD and angiogenesis, we identified proliferative vascular endothelial cells using IF staining for CD31, TGM2, and Ki-67. In the IBD and DSS mouse colitis models, angiogenesis was significantly enhanced, as evidenced by a substantial number of co-stained Ki-67 and TGM2 positive vascular endothelial cells, whereas controls exhibited minimal Ki-67 or TGM2 positive vascular endothelial cells (Fig. 2A–D). These findings support the association between increased TGM2 expression in endothelial cells and angiogenesis in patients with IBD.

To further elucidate the link between TGM2 and angiogenesis, we isolated HIMECs from patients with IBD using enzymatic digestion and magnetic bead sorting (Fig. S2A–C). Lentiviral transfection was performed to manipulate the expression of *TGM2* in HIMECs for subsequent experiments (Fig. S2D–I). *TGM2* knockdown significantly suppressed the tube formation (Fig. 2E), proliferation (Fig. 2F–G), migration (Fig. 2I–J), and invasion (Fig. 2H) of HIMECs in vitro. Conversely, overexpression of *TGM2* markedly enhanced tube formation, migration, and invasion of HIMECs in vitro. These results suggest that TGM2 promotes angiogenesis in patients with IBD by enhancing the tube formation, proliferation, migration, and invasion capabilities of HIMECs.

STAT1-TGM2-VEGFR2 axis drives inflammatory angiogenesis in IBD

To investigate the relationship between TGM2 and inflammatory angiogenesis, HIMECs were stimulated with IL-23 (100 ng/mL), IFN-γ (10 ng/mL), and IL-9 (100 ng/mL), which are crucial in IBD pathogenesis [34]. qPCR analysis and western blotting revealed significant upregulation of *TGM2* mRNA and protein levels in HIMECs upon stimulation with IL-23, IFN-γ, and IL-9 (Fig. 3A–C, Fig. S2K–M). Moreover, an in vitro tube formation assay conducted with HIMECs stimulated with inflammatory factors demonstrated a substantial enhancement in their angiogenic potential compared to controls. Rescue experiments were performed to elucidate the

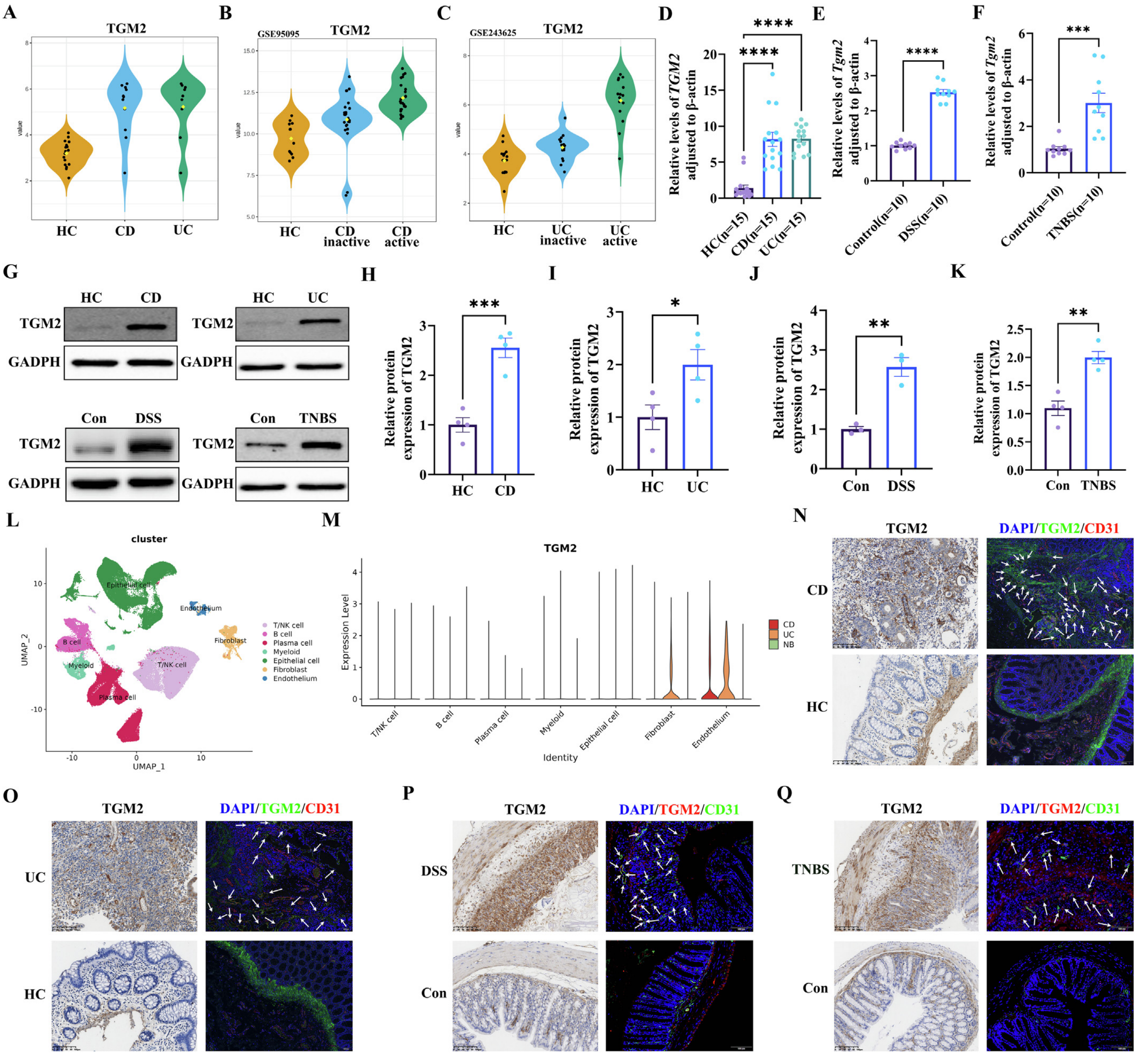

Fig. 1. The expression of TGM2 is increased in enteric endothelial cells of IBD patients and experimental colitis mice. (A) Gene microarray data from our IBD center indicate a significant upregulation in TGM2 expression in IBD patients (HC n = 18, CD n = 12, UC n = 9). (B, C) GEO datasets (GSE95095, GSE243625) also demonstrate a marked upregulation of TGM2 in IBD patients, particularly at the inflamed area. (D) qPCR revealed TGM2 mRNA levels is upregulated in intestinal tissues from IBD patients (n = 15 in each group). (E, F) qPCR revealed TGM2 mRNA levels is elevated in intestinal tissue from DSS and TNBS colitis model (n = 10 in each group). (G-K) The protein level of TGM2 in IBD and colitis model is assessed by WB. The results show that protein level of TGM2 is ascended in IBD and mouse colitis model (n = 4 in each group). (L) The UMAP of different 7 subgroups of total 165,618 cells. (M) The violin plot shows TGM2 is increased in enteric endothelial cells of IBD patients. (N, O) IHC and IF results show significant increase in blood vessel density along with heightened expression levels of TGM2 (green) specifically within CD31 (red) endothelial cells among IBD patients (white arrow). (P, Q) IHC and IF results show prominent upregulation of TGM2 expression in endothelial cells in DSS-induced colitis (white arrow), but only partial co-localization between TGM2 (red) and CD31 (green) within endothelial cells in TNBS colitis (white arrow). (*$p < 0.05$, **$p < 0.01$, ***$p < 0.001$, ****$p < 0.0001$). (For interpretation of the references to colour in this figure legend, the reader is referred to the web version of this article.)

regulatory mechanism underlying IBD-associated inflammatory angiogenesis mediated by TGM2. The knockdown of TGM2 in HIMECs could reverse the effects exerted by IL-23, IFN-γ, and IL-9, which promote tubular structure formation by HIMECs (Fig. 3D). Collectively, these findings suggest that inflammatory factors, such as IL-9, can induce TGM2 expression in HIMECs derived from patients with IBD while promoting angiogenesis.

We further validated the regulatory role of TGM2 in the VEGFR2 pathway. Western blotting results demonstrated that TGM2 significantly augmented VEGFR2 phosphorylation at positions Tyr1059, Tyr1214 (Fig. 3E) and upregulated the phosphorylation of downstream proteins FAK, MAPK, and PLC-γ (Fig. 3F). To elucidate the mechanism by which TGM2 governs the VEGFR2 pathway, we conducted fluorescence co-localization and Co-IP experiments. Co-localization and Co-IP results substantiated an interaction between TGM2 and VEGFR2, thereby confirming that TGM2 may modulate the phosphorylation status of VEGFR2 via protein–protein interactions (Fig. 3G and H).

Using the Gene Transcription Regulation Database (GTRD), we conducted an extensive search for STAT-1 binding sites within a

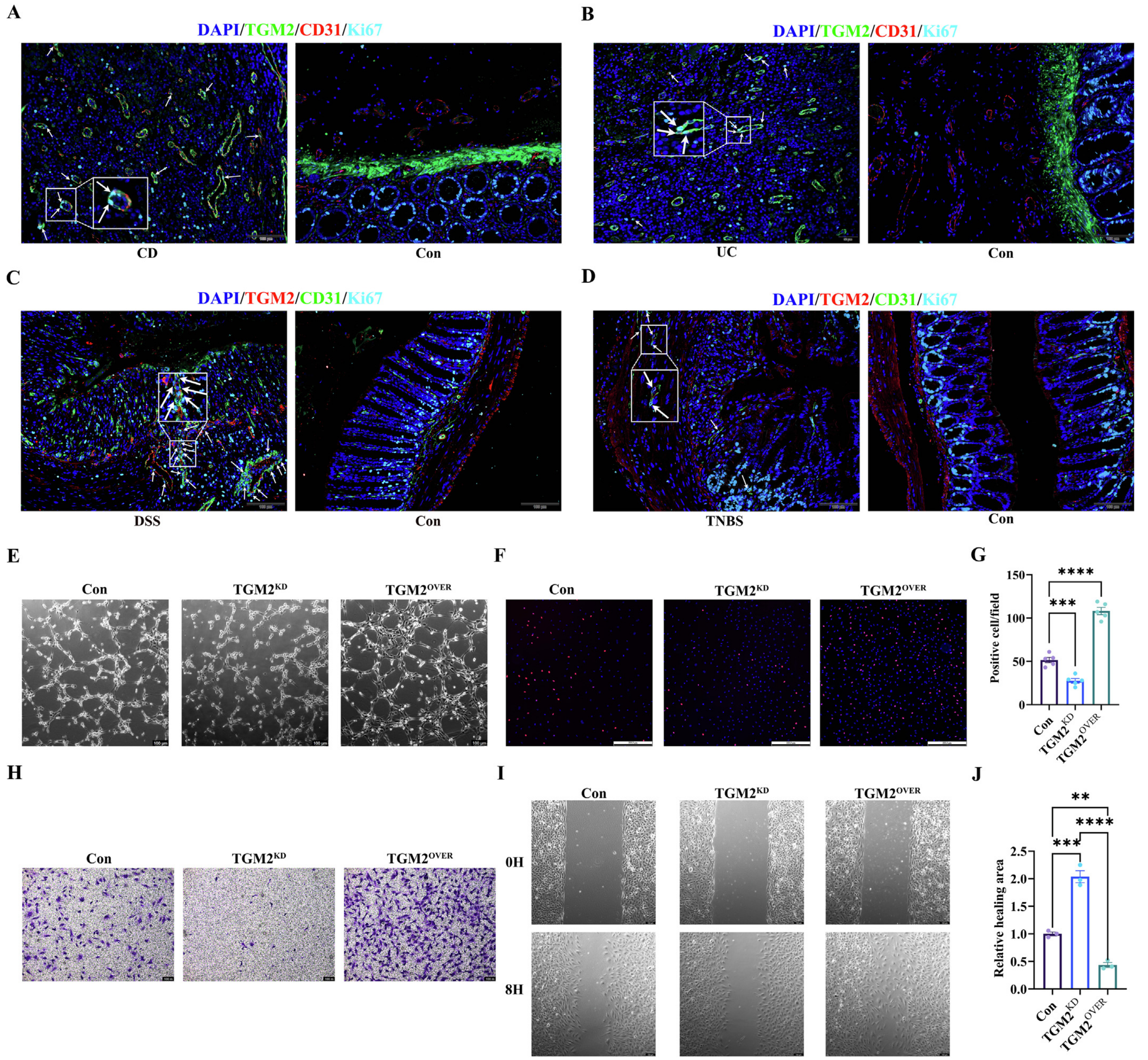

Fig. 2. TGM2 regulates the angiogenic ability of intestinal vascular endothelial cells. (A, B) Multiple immunofluorescence staining for CD31 (red), TGM2 (green), and Ki-67 (cyan) reveals a significant presence of co-stained Ki-67 and TGM2 double positive vascular endothelial cells in patients with CD and UC (White arrow. A representative image of TGM2$^+$ proliferative vascular endothelial cells is displayed within the white frame.). (C, D) The DSS colitis mice exhibit a significant upregulation in the number of CD31 (green), TGM2(red), Ki-67(cyan) positive vascular endothelial cells, whereas this cell is less observed in TNBS colitis mice (White arrow. A representative image of TGM2$^+$ proliferative vascular endothelial cells is displayed within the white frame). (E) The in vitro tube formation assay demonstrated that knockdown of TGM2 significantly attenuated the ability of HIMEC to form tubes, whereas overexpression of TGM2 markedly augmented the tube formation ability of HIMEC. (F, G) EdU proliferation assay showed that TGM2 knockdown significantly inhibited HIMEC proliferation, while TGM2 overexpression significantly enhanced HIMEC proliferation (n = 3 in each group). (H) The Matrigel invasion assay demonstrated that knockdown of TGM2 significantly impeded HIMEC invasion ability, whereas overexpression of TGM2 notable strengthen HIMEC invasion ability. (I, J) The wound healing assay demonstrated a significant reduction in HIMEC migration ability upon inhibition of TGM2, whereas the overexpression of TGM2 significantly enhanced HIMEC migration ability (n = 3 in each group). (*$p < 0.05$, **$p < 0.01$, ***$p < 0.001$, ****$p < 0.0001$). (For interpretation of the references to colour in this figure legend, the reader is referred to the web version of this article.)

2000 kb region upstream of the *TGM2* and identified two regions that exhibited significant enrichment with STAT1 binding sites (Fig. S2J). To elucidate the underlying mechanism by which inflammatory factors promote the upregulation of TGM2 expression, ChIP assays were conducted to validate the specific interactions between STAT1 and the upstream promoter of *TGM2*. The qPCR primers were designed based on the GTRD database results. ChIP results revealed a substantial enrichment of phosphorylated STAT1 (p-STAT1) in both regions containing STAT-1 binding sites within the upstream promoter sequence of *TGM2*. Furthermore, upon treatment with the STAT1 inhibitor fludarabine, a significant reduction in TGM2 protein expression was observed in HIMECs (Fig. S3A and B). These findings strongly suggest that p-STAT1 was recruited to the upstream promoter region of *TGM2* by inflammatory factors to effectively facilitate the transcriptional activation of *TGM2* (Fig. 3I).

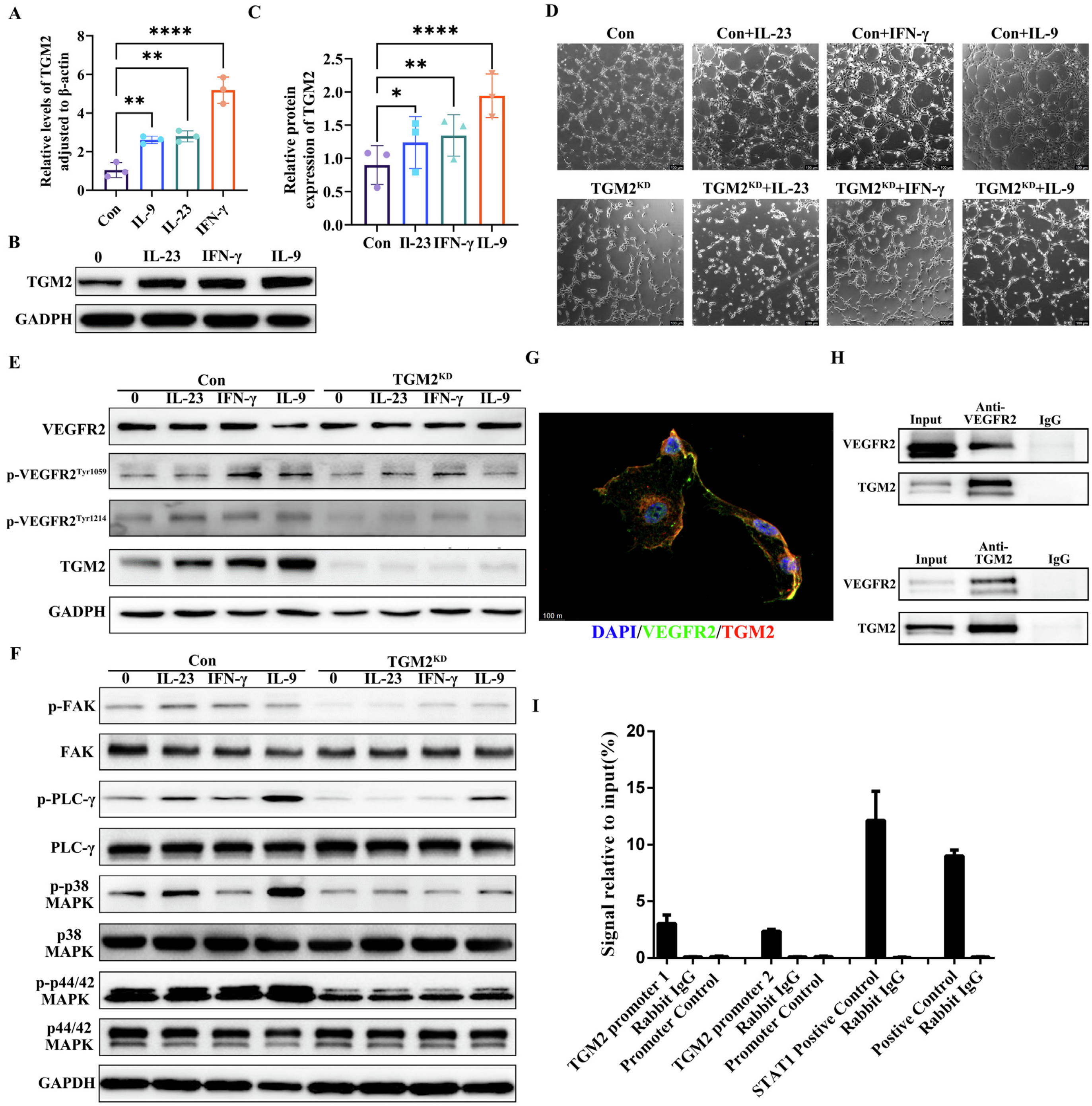

Fig. 3. STAT1-TGM2-VEGFR2 axis drives inflammatory angiogenesis in IBD. (A) The mRNA transcription of TGM2 was significantly upregulated upon stimulation with inflammatory cytokines IL-9, IL-23, and IFN-γ in HIMECs (n = 3 in each group). (B, C) The results of WB demonstrated that stimulation with IL-9, IL-23, and IFN-γ upregulated the protein expression of TGM2 in HIMEC. (D) Stimulation with inflammatory cytokines IL-9, IL-23, and IFN-γ significantly augmented the in vitro angiogenic capacity of HIMECs, while knockdown of TGM2 effectively reversed this effect. (E, F) IL-9, IL-23 and IFN-γ stimulation significantly enhanced the phosphorylation of VEGFR2 at Tyr1059, Tyr1214 and activated the downstream pathways such as FAK, PLC-γ and MAPK pathways in HIMEC, which were reversed by TGM2 knockdown. (G) IF results showed VEGFR2 co-localizes with TGM2 in HIMEC, mainly on the cell membrane. (H) Co-IP results substantiated the interaction between TGM2 and VEGFR2. (I) The CHIP assay confirmed the binding of STAT1 to the upstream promoter region of TGM2, thereby facilitating transcription following IFN-γ stimulation. ($^{*}p < 0.05$, $^{**}p < 0.01$, $^{***}p < 0.001$, $^{****}p < 0.0001$).

Knockout of Tgm2 relieves tissue inflammation and inhibits angiogenesis in DSS colitis model

To further investigate the role of Tgm2 in CD angiogenesis in vivo, we generated mice with *Tgm2* knockout and DSS-induced colitis (Fig. S4A and B). Western blot and IHC analysis confirmed the successful knockout of *Tgm2* (Fig. S4C and D). Compared to the littermate controls, *Tgm2 knockout* mice demonstrated no significant improvement in weight loss (Fig. 4A), colon length (Fig. 4B–C), and DAI score (Fig. 4D). However, H&E staining exhibited a reduced inflammation severity within the *Tgm2* knockout mouse model characterized by reduced ulcer area and infiltration of inflammatory cells (Fig. 4E–F).

Using CD31 as an endothelial marker, we observed decreased vascular density in the *Tgm2* knockout group, suggesting that *Tgm2* knockout reduced angiogenesis in DSS-induced colitis (Fig. 4F, H). The WT-DSS group displayed significantly higher numbers of proliferating vascular endothelial cells than the *Tgm2* knockout group, along with a large number of Ki-67 and TGM2 double-positive endothelial cells, as visualized by IF (Fig. 4I). Western blot analysis was performed to assess the effect of the *Tgm2* knockout on VEGFR2 phosphorylation in acute DSS-induced colitis. The western blotting revealed a reduction in VEGFR2 phosphorylation at Tyr1059 and Tyr1214 in the colonic tissue of mice with *Tgm2* knockout compared to controls (Fig. 4G). These findings indicated that *Tgm2* knockout inhibited angiogenesis in acute DSS-induced colitis by reducing VEGFR2 phosphorylation.

TGM2-specific inhibitor significantly attenuates colitis and angiogenesis in the DSS colitis model

Although *Tgm2* knockout improved colon inflammation and inhibited angiogenesis in mice with acute DSS, no significant improvement was observed in the key indicators of body weight and colon length. We hypothesized that complete and premature inhibition of TGM2 function attributed to *Tgm2* knockdown may impair mucosal healing by entirely impeding angiogenesis. To further explore the potential of drugs targeting TGM2 in IBD treatment, we examined the function of TGM2 in colitis by administering a specific TGM2 inhibitor, GK921, in a DSS model. The cohort that received TGM2 inhibitor treatment exhibited significant improvements in weight loss (Fig. 5A), colon shortening (Fig. 5B–C), and DAI scores (Fig. 5D). Notably, H&E staining revealed a marked reduction in both colitis severity and histological score in the GK921 treatment group (Fig. 5E–F).

We also evaluated the angiogenic effects of TGM2 inhibition using IHC and IF. Using the CD31 antibody for blood vessel labeling, we observed significantly decreased vessel density in the GK921 treatment group, suggesting that TGM2 inhibition can obstruct angiogenesis in the DSS colitis model (Fig. 5F, H). Furthermore, IF results demonstrated that Ki-67-positive vascular endothelial cells were significantly reduced in the GK921 treatment group (Fig. 5I), thereby confirming their efficacy in inhibiting angiogenesis in colitis. In addition, western blotting indicated that the phosphorylation levels of VEGFR2 at Tyr1059 and Tyr1214 were considerably lower in the GK921 treatment group (Fig. 5G). Collectively, these findings indicate that TGM2 inhibitors attenuate angiogenesis via the downregulation of VEGFR2 phosphorylation and could be a potential therapeutic option for IBD.

Serum TGM2 level is a potential biomarker for monitoring endoscopic disease activity in CD

In total, 105 patients diagnosed with CD were enrolled in this study. Of them, 62 exhibited endoscopic activity, whereas 43 demonstrated endoscopic remission. The baseline clinical data are exhibited in Table 1. No differences were noted in sex or age between the endoscopically active and the remission groups. Serum TGM2 concentration was quantified using ELISA. Serum TGM2 levels were considerably higher in patients with CD (Fig. 6A). Serum TGM2 (Fig. 6B), CRP (Fig. 6C), PLT (Fig. 6D), and ESR (Fig. 6E) were markedly elevated in the cohort with endoscopic activity. Furthermore, serum TGM2 (Fig. 6F), CRP (Fig. 6G), PLT (Fig. 6H), and ESR (Fig. 6I) levels exhibited positive correlations with Crohn's Disease Endoscopic Index of Severity (CDEIS). Receiver operating characteristic (ROC) curves were utilized to evaluate the diagnostic utility of plasma TGM2 concentrations and commonly used clinical indicators, including CRP, ESR, and PLT, for assessing endoscopic disease activity (Fig. 6J). Among these indicators, serum TGM2, CRP, and PLT levels demonstrated the potential for monitoring endoscopic disease activity in CD (Table 2). The diagnostic performance of CRP, PLT, and plasma TGM2 concentrations in assessing endoscopic activity in patients with CD was compared utilizing MedCalc software. Serum TGM2 concentration exhibited a higher diagnostic accuracy than CRP and PLT levels. However, there was no significant difference between the diagnostic values of CRP and PLT in terms of their ability to predict endoscopic activity in patients with CD. We also validated the expression levels of TGM2 in the serum of UC patients within a small-scale cohort and observed that the plasma TGM2 concentration in UC patients was significantly elevated compared to the normal control group (Fig. S5A). Additionally, serum TGM2 demonstrated a certain predictive capacity for endoscopic activity in UC patients (Fig. S5B).

Discussion

Angiogenesis is a pivotal process in IBD pathogenesis. However, the precise pathways mediating inflammatory angiogenesis remain unclear. In this study, we observed elevated TGM2 levels in enteric endothelial cells of both patients with IBD and mouse colitis models. Overexpression of TGM2 significantly promoted proliferation, migration, invasion, tube formation, and the VEFGR2 pathway in HIMECs, whereas TGM2 deficiency strongly abrogated these effects. We demonstrated that STAT1 interacted with the TGM2 promoter to upregulate its expression while facilitating VEGFR2 phosphorylation, thus promoting inflammation-associated angiogenesis. *TGM2* knockout or inhibition with GK921 conferred resistance to DSS-induced colitis and alleviated pathological angiogenesis in murine models. Furthermore, elevated levels of TGM2 could effectively distinguish between active and inactive forms of IBD. Collectively, our findings highlight TGM2 as a novel regulator of inflammation-associated angiogenesis and is of great importance in IBD pathogenesis.

Accumulating evidence indicates that angiogenesis contributes significantly to IBD in various inflammatory contexts. Angiogenesis are crucial in IBD pathogenesis [8,10]. It provides a vital blood supply for mucosal healing [35]. It also facilitates the chemotaxis of inflammatory cells and the transport of inflammatory mediators that exacerbate the inflammatory response [36]. Pathological angiogenesis is a critical manifestation of chronic inflammation. These two processes mutually reinforce each other within a vicious cycle throughout the IBD development [37]. However, mechanisms underlying the transition from physiological to pathological angiogenesis in IBD remain largely unknown. Researchers have observed an abnormal increase in microvessel density in inflamed intestinal tissues in patients with IBD [11]. Therefore, a comprehensive investigation of the molecular basis governing inflammatory angiogenesis in IBD may pave the way for novel therapeutic targets aimed at mitigating the effects of IBD.

TGM2 is a versatile protein that crosses diverse cellular compartments under physiological and pathological conditions [14]. It is well-recognized as a component involved in the development of celiac disease [38–40]. The deamidation of gliadin mediated by TGM2 serves as a pivotal factor that initiates the Th1-mediated immune response, ultimately resulting in damage to the intestinal mucosa [39]. Schuppan et al. [40] reported that the TGM2 inhibitor, ZED1227, significantly mitigated gluten-induced duodenal mucosal injury. Our findings indicated that TGM2 was overexpressed and colocalized with CD31 in patients with IBD and mice with colitis. Moreover, TGM2 expression is substantially upregulated in proliferating endothelial cells, suggesting a robust correlation between TGM2 and angiogenesis in patients with IBD.

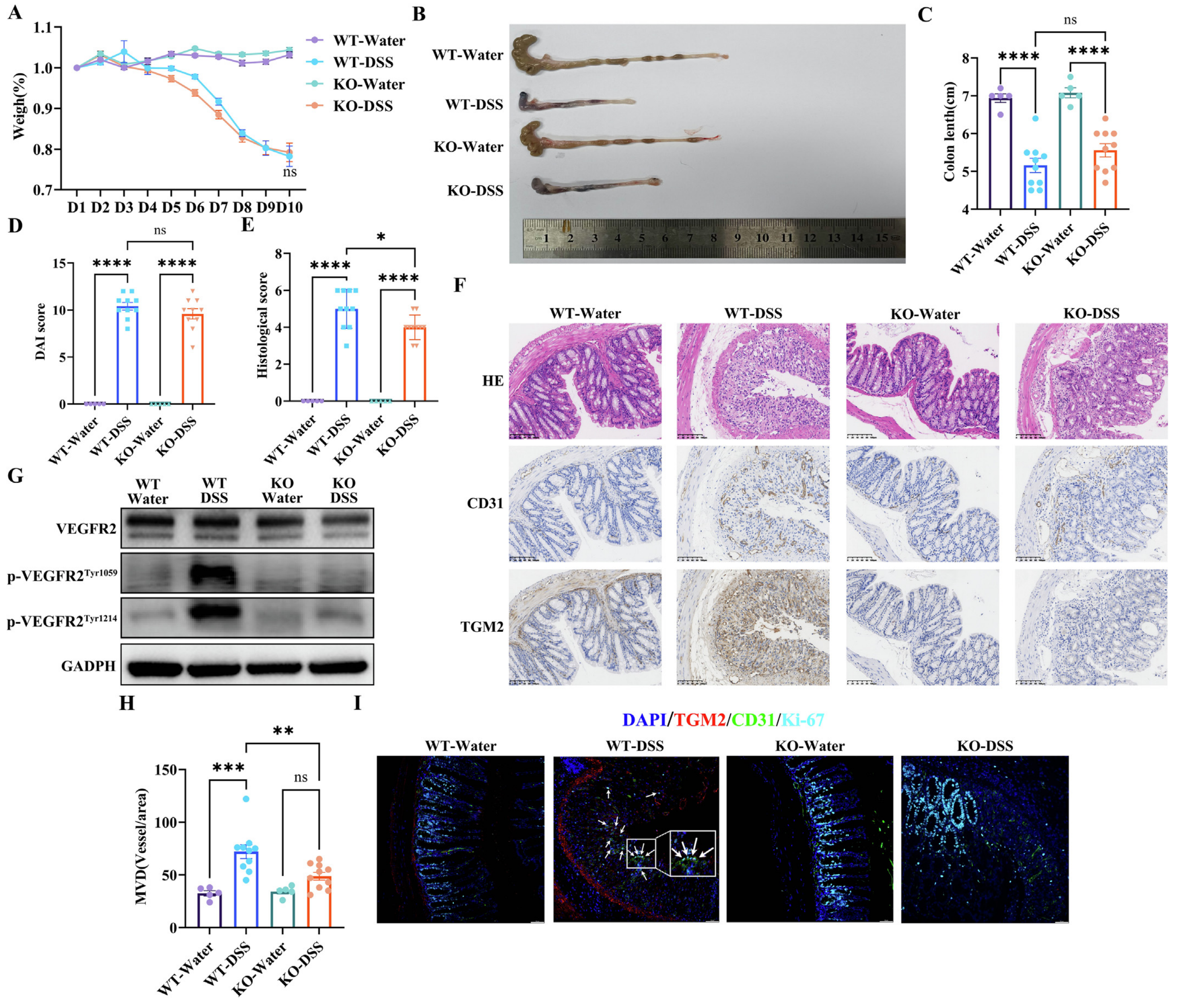

Fig. 4. *Tgm2* knockout relieve tissue inflammation and inhibit angiogenesis in DSS colitis model. (A) Body weight lost of *Tgm2*^{KO} mice and control mice after DSS treatment (n = 5 in WT-Water and KO-Water group, n = 10 in WT-DSS and KO-DSS group). (B) Representative colonic images of DSS-treated *Tgm2*^{KO} mice and control mice. (C) Appearance of colon length of DSS-treated *Tgm2*^{KO} mice and control mice (n = 5 in water group, n = 10 in DSS group,). (D, E) DAI and Histological score of DSS-treated *Tgm2*^{KO} mice and control mice. (n = 5 in water group, n = 10 in DSS group). (F, H) Representative HE staining and Tgm2, CD31 immunohistochemical images of *Tgm2*^{KO} mice and control mice show decreased MVD in *Tgm2*^{KO} mice after DSS treatment. (G)WB result display that *Tgm2*^{KO} mice significantly reduce the phosphorylation of VEGFR2 at Tyr1059 and Tyr1214 after DSS treatment. (I) *Tgm2*^{KO} mice exhibit decrease in the number of Cd31 (green), Tgm2 (red), Ki-67 (cyan) positive proliferative vascular endothelial cells comparing to control mice. ($^{*}p < 0.05$, $^{**}p < 0.01$, $^{***}p < 0.001$, $^{****}p < 0.0001$). (For interpretation of the references to colour in this figure legend, the reader is referred to the web version of this article.)

The establishment of the intestinal microcirculation requires a series of highly specialized cellular systems and is intricately linked to pathological conditions, including inflammation and injury [9]. Previous studies have characterized the role of TGM2 in HUVECs [41]. However, endothelial cells from various tissues display distinct biological characteristics and respond differently to diverse stimuli. Consequently, studies focusing on HUVECs are limited in their applicability for examining the functions of tissue-specific endothelial cells. We isolated and cultured primary HIMECs from the surgical tissues of patients with IBD. Knockdown and overexpression of TGM2 proved that TGM2 regulated the angiogenic ability of HIMECs. More importantly, TGM2 knockdown strongly reversed the proangiogenic effects of proinflammatory cytokines in HIMECs, indicating that TGM2 plays a crucial role in inflammatory angiogenesis in IBD.

Inflammatory stimuli activate HIMECs and induce phosphorylation of VEGFR2, thereby facilitating angiogenesis through downstream signaling pathways [42]. VEGF and its receptor VEGFR2 serve as crucial regulators of neovascularization and remodeling of the existing vasculature within tissues [43]. The activation of VEGFR2 stimulates intracellular signaling pathways that are essential for determining the fate of vascular endothelial cells [43]. VEGFR2 and its downstream signaling cascades are crucial in angiogenesis in patients with IBD [8,42]. Notably, the activation of the VEGFR2 pathway has been confirmed in the inflamed mucosa of patients with IBD, and curcumin inhibits VEGFA-

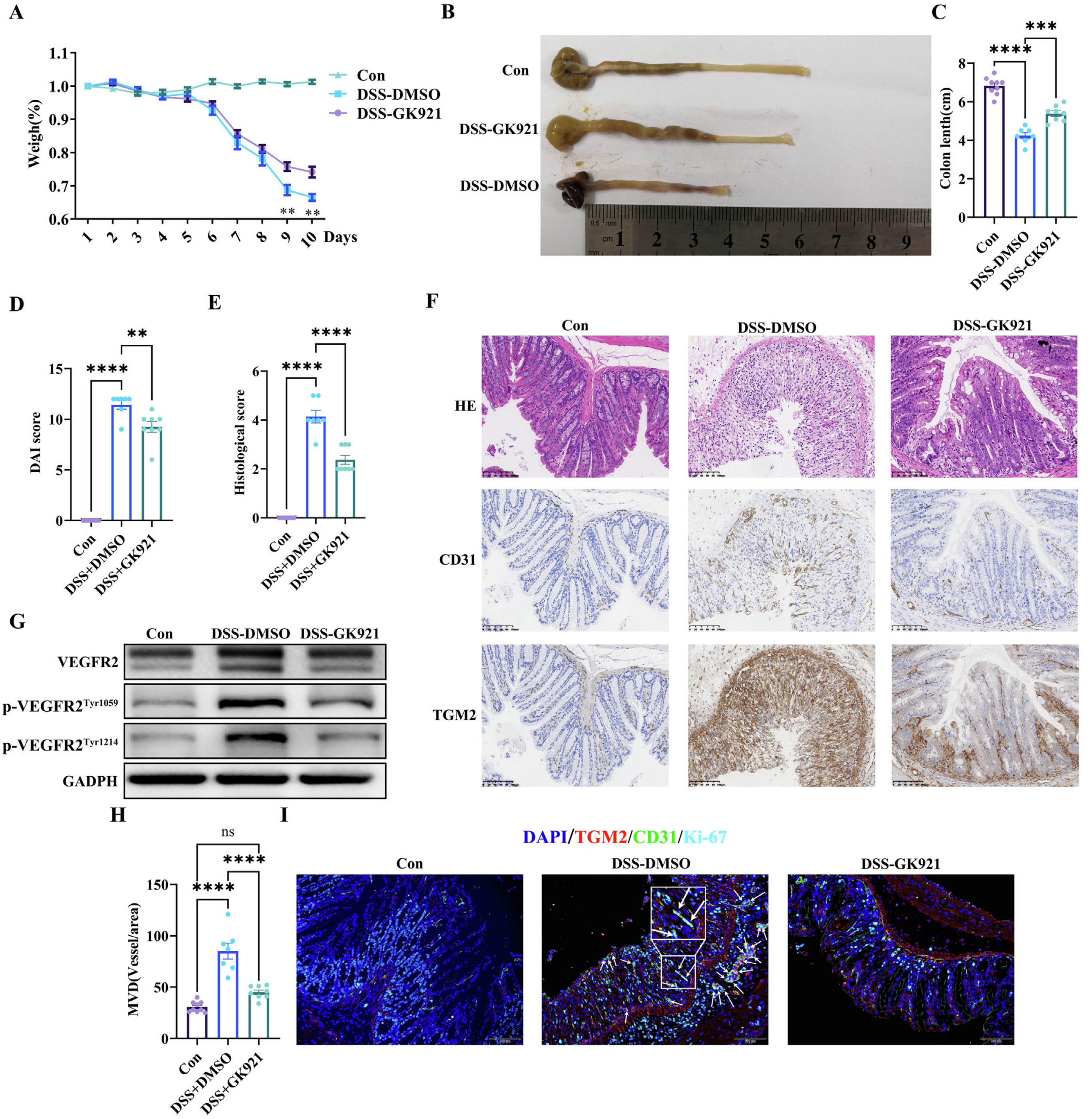

Fig. 5. TGM2 specific inhibitor significantly attenuates colitis and angiogenesis in DSS colitis model. (A) Body lost of GK921 treatment group and solvent treatment group after DSS colitis model establishment (n = 9 in Con group, n = 7 in DSS-DMSO, n = 8 in DSS-GK921 treatment group). (B) Representative colonic images of GK921 treatment group and solvent treatment group after DSS colitis model establishment. (C) Appearance of colon length of GK921 treatment group and solvent treatment group after DSS establishment (n = 9 in Con group, n = 7 in DSS-DMSO, n = 8 in DSS-GK921 treatment group). (D, E) DAI and CDMI score of GK921 treatment group and solvent treatment group after DSS colitis model establishment (n = 9 in Con group, n = 7 in DSS-DMSO, n = 8 in DSS-GK921 treatment group). (F, H) Representative HE staining and TGM2, CD31 immunohistochemical images of GK921 treatment group and solvent treatment group after DSS colitis model establishment show decreased MVD in DSS mice after GK921 treatment. (G) WB result display that GK921 treatment significantly reduce the phosphorylation of VEGFR2 at Tyr1059 and Tyr1214 after DSS treatment. (I) GK921 treatment exhibit decrease in the number of CD31 (green), TGM2 (red), Ki-67 (cyan) positive proliferative vascular endothelial cells comparing to controls. ($^{*}p < 0.05$, $^{**}p < 0.01$, $^{***}p < 0.001$, $^{****}p < 0.0001$). (For interpretation of the references to colour in this figure legend, the reader is referred to the web version of this article.)

mediated tube formation in HIMECs by suppressing the COX-2 and MAPK pathways [44]. However, the precise mechanism by which the intestinal microenvironment activates the VEGFR2 pathway in patients with IBD remains poorly elucidated. In this study, we found that TGM2 interacted with VEGFR2 in HIMECs via co-immunoprecipitation. Treatment with inflammatory stimuli resulted in increased phosphorylation of VEGFR2 in HIMECs, which was significantly reversed by the knockdown of endogenous *TGM2* expression. Specifically, TGM2-induced phosphorylation of VEGFR2 and downstream phosphorylation events involved FAK,

Table 1
Basic clinical characteristics of patients with CD.

Baseline and clinical data	Patients with CD(n = 105)
Median age, yr, (IQR)	28(16.5)
Sex, n (%)	
Male	70(66.7 %)
Female	35(33.3 %)
Age of diagnosis(A), n (%)	
≤16 years old(A1)	11(10.5 %)
16–40 years old(A2)	76(72.4 %)
≥40 years old(A3)	18(17.1 %)
Disease location(L), n (%)	
Terminal ileum(L1)	10(9.5 %)
Colon(L2)	5(4.8 %)
Ileocolon(L3)	90(85.7 %)
Upper GI location(L4)	18(17.1 %)
Perianal fistulae and abscesses(p)	40(38.1 %)
Disease behaviour, n (%)	
Non-stricturing non-penetrating(B1)	58(55.2 %)
Stricturing(B2)	26(24.8 %)
Penetrating(B3)	21(20.0 %)
Medication, n (%)	
Glucocorticoid	22(21.0 %)
Immunosuppressor	27(25.7 %)
Biologicals	16(15.2 %)
Thalidomide	7(6.7 %)
Total Enteral Nutrition Therapy	5(4.8 %)
Mesalazine	13(12.4 %)
Other	15(14.3 %)

MAPK, and PLC-γ pathways. These findings suggest that TGM2 facilitates angiogenesis by activating VEGFR2 and its associated downstream signaling in HIMECs. We also examined potential upstream regulatory mechanisms governing TGM2 expression. We identified potential transcription factor-binding sites located within 2000-bp upstream of the TGM2 start codon and uncovered two enriched regions containing STAT1 binding sites utilizing the GTRD database [45]. ChIP validated the binding of STAT1 to the TGM2 promoter. Therefore, we conclude that TGM2 exerted pro-inflammatory and angiogenic activities in IBD.

Emerging evidence has highlighted angiogenesis as a promising therapeutic target for IBD. Monoclonal antibodies targeting VEGFR have demonstrated significant efficacy in murine colitis [46]. However, case reports have documented instances of exacerbated colitis in patients with colitis-associated colon cancer treated with bevacizumab or sorafenib [47,48]. We generated mice with *TGM2* knockout to determine whether TGM2 is a potential therapeutic target in IBD. Although *TGM2* knockout improved colon inflammation and inhibited angiogenesis under conditions involving acute DSS, no significant difference was found in the key indicator of mouse body weight. We hypothesized that TGM2 knockdown might lead to impaired mucosal healing due to the premature and complete inhibition of TGM2 function and blocked angiogenesis. While TGM2 knockout improved histology by suppressing pathological angiogenesis in acute DSS colitis, the absence of improvement in weight loss or colon length indicates impaired mucosal repair. This aligns with our mechanistic understanding that complete genetic ablation disrupts both pathological and physiological TGM2 functions, resulting in mucosal healing disorders. In contrast, pharmacological TGM2 inhibition significantly improved all metrics, including weight loss, colon shortening length, inflammation, and histopathology, with greater efficacy than knockout. This differential efficacy stems from the partial TGM2 suppression achieved by inhibitors, rather than complete TGM2 suppression, which preserves its physiological function essential for mucosal repair while still blocking pathological angiogenesis. Collectively, these data highlight that therapeutic efficacy requires precise modulation of TGM2 activity. Future TGM2-targeted strategies for IBD must balance angiogenesis inhibition with preservation of healing capacity, potentially through dose optimization or tissue-selective delivery. This finding also indicates that the timing and extent of angiogenesis inhibition should be meticulously regulated when using antiangiogenic agents in the treatment of IBD. Given the ubiquitous expression of TGM2, systemic inhibition inevitably entails risks of off-target effects, particularly impaired wound healing, diarrhoea, vomiting and abdominal pain, as observed in the human clinical trial of TGM2 inhibitor [40]. Although pharmacological inhibition may partially preserve physiological TGM2 functions due to incomplete target suppression, the risk of delayed healing remains a substantial barrier to clinical translation. In light of these challenges, further research, such as tissue-selective delivery strategies, is essential to resolve the trade-off between suppressing pathological TGM2 activity and maintaining its tissue-repair functions.

Currently, the therapeutic focus for IBD has transitioned from symptomatic relief to mucosal healing, rendering the monitoring of endoscopic disease activity a paramount priority in disease management [49]. Although colonoscopy is considered the gold standard for diagnosing and evaluating the degree of endoscopic activity during IBD follow-up, its application is limited by its invasive nature, suboptimal patient compliance, and the need to weigh the benefits of repeated endoscopic assessments against potential risks such as bowel perforation and bleeding [50,51]. In recent studies, fecal calprotectin and cross-sectional imaging have emerged as viable alternatives to colonoscopy for both diagnosis and longitudinal evaluation of IBD [51,52]. Given the persistent challenges related to cost-effectiveness and inter-observer variability, there is an increasing demand for more standardized, cost-efficient, and time-effective monitoring strategies for assessing disease activity in IBD. In this context, we found TGM2 as a novel serological biomarker that may be instrumental in monitoring endoscopic disease activity in patients with CD. Serum TGM2 concentrations were substantially higher in patients exhibiting endoscopic activity than those in remission or healthy controls. TGM2 levels showed substantial positive correlation with clinical indices such as CDAI and CDEIS, was observed, suggesting that TGM2 could serve as an indicator of disease progression. Further, plasma TGM2 concentration demonstrated superior diagnostic efficacy relative to commonly used clinical indicators such as CRP, indicating that it may represent a promising candidate for monitoring endoscopic disease activity in patients with IBD.

Although our study provides novel insights, several limitations should be noted. First, previous studies have demonstrated that TGM2 expressed in macrophages and fibroblasts plays a regulatory role in tumor angiogenesis [53,54]. While our scRNA-seq data from publicly available databases revealed predominant TGM2 upregulation in endothelial cells, its potential roles in other cell types, such as macrophages or fibroblasts, warrant further investigation. Second, the specific binding sites and interaction mechanisms between VEGFR2 and TGM2 have yet to be fully elucidated. Additional experiments, such as introducing point mutations or developing targeted inhibitors to specifically disrupt the TGM2-VEGFR2 interaction, could provide more definitive evidence that TGM2 binding to VEGFR2 promotes angiogenesis in IBD. Furthermore, mechanistic investigations involving the reintroduction of TGM2 in KO mice or HIMECs would help elucidate the functional significance of the TGM2-VEGFR2 binding in angiogenesis, substantially strengthening the robustness and persuasiveness of the conclusions. In addition, this study was conducted at a single center and may therefore be subject to certain selection biases and limitations. Hence, large-scale, multi-center prospective studies are warranted in the future to further validate the clinical utility of TGM2 in monitoring endoscopic activity in patients with IBD.

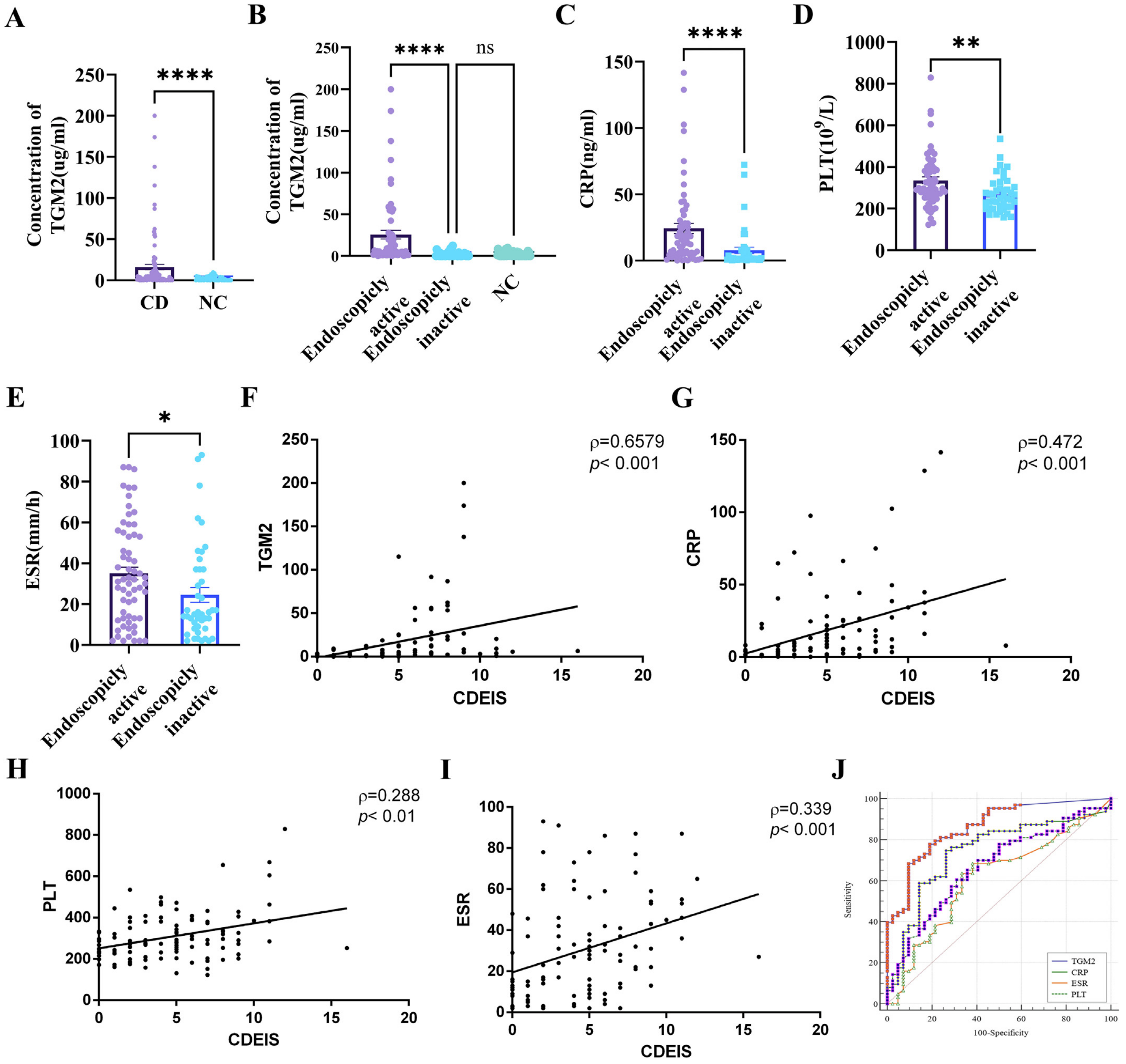

Fig. 6. Serum TGM2 is a potential biomarker for monitoring endoscopic disease activity in CD. (A) Serum TGM2 concentrations were significantly increased in CD patients. (B-E) Levels of serum TGM2, CRP, PLT and ESR were markedly elevated in the endoscopically active cohort. (F-I) Serum TGM2, CRP, PLT and ESR exhibited positive correlations with CDEIS. (J) ROC curves of serum TGM2, CRP and PLT in assessing endoscopic disease activity show serum TGM2 is a reliable biomarker for monitoring endoscopic disease activity in CD. (**p* < 0.05, ***p* < 0.01, ****p* < 0.001, *****p* < 0.0001).

Table 2
Efficiency of TGM2 and other indices for endoscopic evaluation.

Biomarker	Cut-off	AUROC	Se	Spe	p value
TGM2	>2.87 ng/ml	0.862	77.78	80.95	p < 0.001
CRP	>5mg/L	0.74	74.6	73.81	p < 0.001
PLT	>276	0.668	65.08	64.29	p < 0.01
ESR	–	–	–	–	0.507

Conclusions

In summary, we identified TGM2, as not only a potential biomarker for monitoring endoscopic disease activity in IBD but also as a target for promoting angiogenesis under conditions involving intestinal inflammation via the STAT1-TGM2-VEGFR2 axis and its downstream effectors in patients with IBD. Our study enhances our understanding of the molecular pathogenesis of IBD and demonstrates that TGM2 may play a pivotal role in this condition. Furthermore, inhibition of TGM2 could lead to therapeutic benefits in the management of IBD, thereby establishing a foundation for examining TGM2 as a therapeutic target to develop innovative treatments for this disorder.

Compliance with ethics requirement

All Institutional and National Guidelines for the care and use of human or animal subjects were followed.

Declaration of competing interest

The authors declare that they have no known competing financial interests or personal relationships that could have appeared to influence the work reported in this paper.

Acknowledgments

This study was supported by National Key R&D Program of China (2023YFC2507300), Guangdong Basic and Applied Basic Research Foundation (#2024A1515013032, #2024A1515012956), the National Natural Science Foundation of China (#82470548, #82100572, #82270555), the China Postdoctoral Science Foundation (#2019M653228), and Guangdong Province Higher Vocational Colleges & Schools Pearl River Scholar Funded Scheme 2024.

Appendix A. Supplementary material

Supplementary data to this article can be found online at https://doi.org/10.1016/j.jare.2025.07.002.

References

[1] Roda G, Chien Ng S, Kotze PG, Argollo M, Panaccione R, Spinelli A, et al. Crohn's disease, nature reviews. Disease Primers 2020;6(1):22. doi: https://doi.org/10.1038/s41572-020-0156-2.

[2] Kobayashi T, Siegmund B, Le Berre C, Wei SC, Ferrante M, Shen B, et al. Ulcerative colitis, Nature reviews. Disease primers 2020;6(1):74. doi: https://doi.org/10.1038/s41572-020-0205-x.

[3] Liu J, Di B, Xu LL. Recent advances in the treatment of IBD: targets, mechanisms and related therapies. Cytokine Growth Fact Rev 2023;71–72:1–12. doi: https://doi.org/10.1016/j.cytogfr.2023.07.001.

[4] Vieujean S, D'Amico F, Netter P, Danese S, Peyrin-Biroulet L. Landscape of new drugs and targets in inflammatory bowel disease. United European Gastroenterol J 2022;10(10):1129–66. doi: https://doi.org/10.1002/ueg2.12305.

[5] D'Alessio S, Tacconi C, Fiocchi C, Danese S. Advances in therapeutic interventions targeting the vascular and lymphatic endothelium in inflammatory bowel disease. Curr. Opin. Gastroenterol. 2013;29(6):608–13. doi: https://doi.org/10.1097/MOG.0b013e328365d37c.

[6] Wang SS, Zhu XX, Wu XY, Zhang WW, Ding YD, Jin SW, et al. Interaction between blood vasculatures and lymphatic vasculatures during inflammation. J Inflamm Res 2023;16:3271–81. doi: https://doi.org/10.2147/jir.S414891.

[7] Chang JT. Pathophysiology of inflammatory bowel diseases. New England J Med 2020;383(27):2652–64. doi: https://doi.org/10.1056/NEJMra2002697.

[8] Danese S, Sans M, de la Motte C, Graziani C, West G, Phillips MH, et al. Angiogenesis as a novel component of inflammatory bowel disease pathogenesis. Gastroenterology 2006;130(7):2060–73. doi: https://doi.org/10.1053/j.gastro.2006.03.054.

[9] Danese S. Role of the vascular and lymphatic endothelium in the pathogenesis of inflammatory bowel disease: 'brothers in arms'. Gut 2011;60(7):998–1008. doi: https://doi.org/10.1136/gut.2010.207480.

[10] Alkim C, Alkim H, Koksal AR, Boga S, Sen I. Angiogenesis in inflammatory bowel disease. Int J Inflamm 2015;2015:970890. doi: https://doi.org/10.1155/2015/970890.

[11] Deban L, Correale C, Vetrano S, Malesci A, Danese S. Multiple pathogenic roles of microvasculature in inflammatory bowel disease: a Jack of all trades. Am J Pathol 2008;172(6):1457–66. doi: https://doi.org/10.2353/ajpath.2008.070593.

[12] Binion DG, Rafiee P. Is inflammatory bowel disease a vascular disease? Targeting angiogenesis improves chronic inflammation in inflammatory bowel disease. Gastroenterology 2009;136(2):400–3. doi: https://doi.org/10.1053/j.gastro.2008.12.029.

[13] Lee CS, Park HH. Structural aspects of transglutaminase 2: functional, structural, and regulatory diversity. Apopt Int J Program Cell Death 2017;22(9):1057–68. doi: https://doi.org/10.1007/s10495-017-1396-9.

[14] Yao Z, Fan Y, Lin L, Kellems RE, Xia Y. Tissue transglutaminase: a multifunctional and multisite regulator in health and disease. Physiol Rev 2024;104(1):281–325. doi: https://doi.org/10.1152/physrev.00003.2023.

[15] Zaltron E, Vianello F, Ruzza A, Palazzo A, Brillo V, Celotti I, et al. The role of transglutaminase 2 in cancer: an update. Int J Mol Sci 2024;25(5). doi: https://doi.org/10.3390/ijms25052797.

[16] Wang Z, Perez M, Lee ES, Kojima S, Griffin M. The functional relationship between transglutaminase 2 and transforming growth factor β1 in the regulation of angiogenesis and endothelial-mesenchymal transition. Cell Death Dis 2017;8(9):e3032.

[17] Lee SH, Kang JH, Ha JS, Lee JS, Oh SJ, Choi HJ, et al. Transglutaminase 2-mediated p53 depletion promotes angiogenesis by increasing HIF-1α-p300 binding in renal cell carcinoma. Int J Mol Sci 2020;21(14). doi: https://doi.org/10.3390/ijms21145042.

[18] Asad S, Wegler C, Ahl D, Bergström CAS, Phillipson M, Artursson P, et al. Proteomics-informed identification of luminal targets for in situ diagnosis of inflammatory bowel disease. J Pharm Sci 2021;110(1):239–50. doi: https://doi.org/10.1016/j.xphs.2020.11.001.

[19] Elli L, Ciulla MM, Busca G, Roncoroni L, Maioli C, Ferrero S, et al. Beneficial effects of treatment with transglutaminase inhibitor cystamine on the severity of inflammation in a rat model of inflammatory bowel disease. Laborat Invest; A J Technical Methods Pathol 2011;91(3):452–61. doi: https://doi.org/10.1038/labinvest.2010.186.

[20] Jeong EM, Son YH, Choi Y, Kim JH, Lee JH, Cho SY, et al. Transglutaminase 2 is dispensable but required for the survival of mice in dextran sulfate sodium-induced colitis. Exp Mol Med 2016;48(11):e267.

[21] Magro F, Gionchetti P, Eliakim R, Ardizzone S, Armuzzi A, Barreiro-de Acosta M, et al. Third European evidence-based consensus on diagnosis and management of ulcerative colitis. Part 1: definitions, diagnosis, extra-intestinal manifestations, pregnancy, cancer surveillance, surgery, and Ileo-anal pouch disorders. J Crohns Colitis 2017;11(6):649–70. doi: https://doi.org/10.1093/ecco-jcc/jjx008.

[22] Mary JY, Modigliani R. Development and validation of an endoscopic index of the severity for Crohn's disease: a prospective multicentre study. Groupe d'Etudes Thérapeutiques des Affections Inflammatoires du Tube Digestif (GETAID). Gut 1989;30(7):983–9. doi: https://doi.org/10.1136/gut.30.7.983.

[23] Gomollón F, Dignass A, Annese V, Tilg H, Van Assche G, Lindsay JO, et al. 3rd European evidence-based consensus on the diagnosis and management of Crohn's disease 2016: Part 1: diagnosis and medical management. J Crohns Colitis 2017;11(1):3–25. doi: https://doi.org/10.1093/ecco-jcc/jjw168.

[24] Liu P, Ewald J, Pang Z, Legrand E, Jeon YS, Sangiovanni J, et al. Express analyst: a unified platform for RNA-sequencing analysis in non-model species. Nat Commun 2023;14(1):2995. doi: https://doi.org/10.1038/s41467-023-38785-y.

[25] Martin JC, Chang C, Boschetti G, Ungaro R, Giri M, Grout JA, et al. Single-cell analysis of Crohn's disease lesions identifies a pathogenic cellular module associated with resistance to anti-TNF therapy. Cell 2019;178(6):1493–1508.e20. doi: https://doi.org/10.1016/j.cell.2019.08.008.

[26] Maddipatla SC, Kolachala VL, Venkateswaran S, Dodd AF, Pelia RS, Geem D, et al. Assessing cellular and transcriptional diversity of Ileal Mucosa among treatment-Naïve and treated Crohn's disease. Inflamm Bowel Dis 2023;29(2):274–85. doi: https://doi.org/10.1093/ibd/izac201.

[27] Garrido-Trigo A, Corraliza AM, Veny M, Dotti I, Melón-Ardanaz E, Rill A, et al. Macrophage and neutrophil heterogeneity at single-cell spatial resolution in human inflammatory bowel disease. Nat Commun 2023;14(1):4506. doi: https://doi.org/10.1038/s41467-023-40156-6.

[28] Du J, Zhang J, Wang L, Wang X, Zhao Y, Lu J, et al. Selective oxidative protection leads to tissue topological changes orchestrated by macrophage during ulcerative colitis. Nat Commun 2023;14(1):3675. doi: https://doi.org/10.1038/s41467-023-39173-2.

[29] Hao Y, Hao S, Andersen-Nissen E, Mauck 3rd WM, Zheng S, Butler A, et al. Integrated analysis of multimodal single-cell data. Cell 2021;184(13):3573–3587.e29. doi: https://doi.org/10.1016/j.cell.2021.04.048.

[30] Wickham H, Averick M, Bryan J, Chang W, McGowan L, François R, et al. Welcome to the Tidyverse. J Open Source Soft 2019;4(43). doi: https://doi.org/10.21105/joss.01686.

[31] Wirtz S, Popp V, Kindermann M, Gerlach K, Weigmann B, Fichtner-Feigl S, et al. Chemically induced mouse models of acute and chronic intestinal inflammation. Nat. Protoc. 2017;12(7):1295–309. doi: https://doi.org/10.1038/nprot.2017.044.

[32] Binion DG, West GA, Ina K, Ziats NP, Emancipator SN, Fiocchi C. Enhanced leukocyte binding by intestinal microvascular endothelial cells in inflammatory bowel disease. Gastroenterology 1997;112(6):1895–907. doi: https://doi.org/10.1053/gast.1997.v112.pm9178682.

[33] Wang Y, Han J, Yang G, Zheng S, Zhou G, Liu X, et al. Therapeutic potential of the secreted Kazal-type serine protease inhibitor SPINK4 in colitis. Nat. Commun. 2024;15(1):5874. doi: https://doi.org/10.1038/s41467-024-50048-y.

[34] Neurath MF. Strategies for targeting cytokines in inflammatory bowel disease. Nat RevImmunol. 2024;24(8):559–76. doi: https://doi.org/10.1038/s41577-024-01008-6.

[35] Sajib S, Zahra FT, Lionakis MS, German NA, Mikelis CM. Mechanisms of angiogenesis in microbe-regulated inflammatory and neoplastic conditions.

Angiogenesis 2018;21(1):1–14. doi: https://doi.org/10.1007/s10456-017-9583-4.

[36] Li Y, Zhu W, Zuo L, Shen B. The role of the mesentery in crohn's disease: the contributions of nerves, vessels, lymphatics, and fat to the pathogenesis and disease course. Inflamm Bowel Dis 2016;22(6):1483–95. doi: https://doi.org/10.1097/mib.0000000000000791.

[37] Chidlow Jr JH, Shukla D, Grisham MB, Kevil CG. Pathogenic angiogenesis in IBD and experimental colitis: new ideas and therapeutic avenues. Am J Physiol Gastrointest Liver Physiol 2007;293(1):G5–g18. doi: https://doi.org/10.1152/ajpgi.00107.2007.

[38] Dieterich W, Ehnis T, Bauer M, Donner P, Volta U, Riecken EO, et al. Identification of tissue transglutaminase as the autoantigen of celiac disease. Nat Med 1997;3(7):797–801. doi: https://doi.org/10.1038/nm0797-797.

[39] Arentz-Hansen H, Körner R, Molberg O, Quarsten H, Vader W, Kooy YM, et al. The intestinal T cell response to alpha-gliadin in adult celiac disease is focused on a single deamidated glutamine targeted by tissue transglutaminase. J Exp Med 2000;191(4):603–12. doi: https://doi.org/10.1084/jem.191.4.603.

[40] Schuppan D, Mäki M, Lundin KEA, Isola J, Friesing-Sosnik T, Taavela J, et al. A randomized trial of a transglutaminase 2 inhibitor for celiac disease. New Engl J Med 2021;385(1):35–45. doi: https://doi.org/10.1056/NEJMoa2032441.

[41] Wang Z, Perez M, Caja S, Melino G, Johnson TS, Lindfors K, et al. A novel extracellular role for tissue transglutaminase in matrix-bound VEGF-mediated angiogenesis. Cell Death Dis 2013;4(9):e808.

[42] Scaldaferri F, Vetrano S, Sans M, Arena V, Straface G, Stigliano E, et al. VEGF-A links angiogenesis and inflammation in inflammatory bowel disease pathogenesis 585-95.e5. Gastroenterology 2009;136(2). doi: https://doi.org/10.1053/j.gastro.2008.09.064.

[43] Simons M, Gordon E, Claesson-Welsh L. Mechanisms and regulation of endothelial VEGF receptor signalling. Nat Rev Mol Cell Biol 2016;17(10):611–25. doi: https://doi.org/10.1038/nrm.2016.87.

[44] Binion DG, Otterson MF, Rafiee P. Curcumin inhibits VEGF-mediated angiogenesis in human intestinal microvascular endothelial cells through COX-2 and MAPK inhibition. Gut 2008;57(11):1509–17. doi: https://doi.org/10.1136/gut.2008.152496.

[45] Kolmykov S, Yevshin I, Kulyashov M, Sharipov R, Kondrakhin Y, Makeev VJ, et al. GTRD: an integrated view of transcription regulation. Nucleic Acids Res 2021;49(D1):D104–11. doi: https://doi.org/10.1093/nar/gkaa1057.

[46] Knod L, Donovan EC, Chernoguz A, Crawford KM, Dusing MR, Frischer JS. Vascular endothelial growth factor receptor-2 inhibition in experimental murine colitis. J Surg Res 2013;184(1):101–7. doi: https://doi.org/10.1016/j.jss.2013.04.026.

[47] Adenis A, Vanseymortier L, Foissey D, Colombel JF. Bevacizumab and postponed suture leakages after surgery for ulcerative colitis and rectal cancer. Gut 2007;56(5):734. doi: https://doi.org/10.1136/gut.2006.112524.

[48] Loriot Y, Boudou-Rouquette P, Billemont B, Ropert S, Goldwasser F. Acute exacerbation of hemorrhagic rectocolitis during antiangiogenic therapy with sunitinib and sorafenib. Ann Oncol: Off J Eur Soc Med Oncol 2008;19(11):1975. doi: https://doi.org/10.1093/annonc/mdn566.

[49] Turner D, Ricciuto A, Lewis A, D'Amico F, Dhaliwal J, Griffiths AM, et al. STRIDE-II: an Update on the Selecting Therapeutic Targets in Inflammatory Bowel Disease (STRIDE) Initiative of the International Organization for the Study of IBD (IOIBD): determining Therapeutic Goals for Treat-to-Target strategies in IBD. Gastroenterology 2021;160(5):1570–83. doi: https://doi.org/10.1053/j.gastro.2020.12.031.

[50] West J, Tan K, Devi J, Macrae F, Christensen B, Segal JP. Benefits and challenges of treat-to-target in inflammatory bowel disease. J Clin Med 2023;12(19). doi: https://doi.org/10.3390/jcm12196292.

[51] Rimola J, Torres J, Kumar S, Taylor SA, Kucharzik T. Recent advances in clinical practice: advances in cross-sectional imaging in inflammatory bowel disease. Gut 2022;71(12):2587–97. doi: https://doi.org/10.1136/gutjnl-2021-326562.

[52] Bohra A, Mohamed G, Vasudevan A, Lewis D, Van Langenberg DR, Segal JP. The utility of faecal calprotectin, lactoferrin and other faecal biomarkers in discriminating endoscopic activity in Crohn's disease: a systematic review and meta-analysis. Biomedicines 2023;11(5). doi: https://doi.org/10.3390/biomedicines11051408.

[53] Moradi-Chaleshtori M, Koochaki A, Shojaei S, Paryan M, Safarzadeh M, Hashemi SM, et al. Overexpression of pigment epithelium-derived factor in breast cancer cell-derived exosomes induces M1 polarization in macrophages. Immunol Lett 2022;248:31–6. doi: https://doi.org/10.1016/j.imlet.2022.05.005.

[54] Hernandez-Fernaud JR, Ruengeler E, Casazza A, Neilson LJ, Pulleine E, Santi A, et al. Secreted CLIC3 drives cancer progression through its glutathione-dependent oxidoreductase activity. Nat. Commun. 2017;8:14206. doi: https://doi.org/10.1038/ncomms14206.